eLIFE
elifesciences.org

Figures and figure supplements

Designed α-sheet peptides inhibit amyloid formation by targeting toxic oligomers

Gene Hopping, et al.

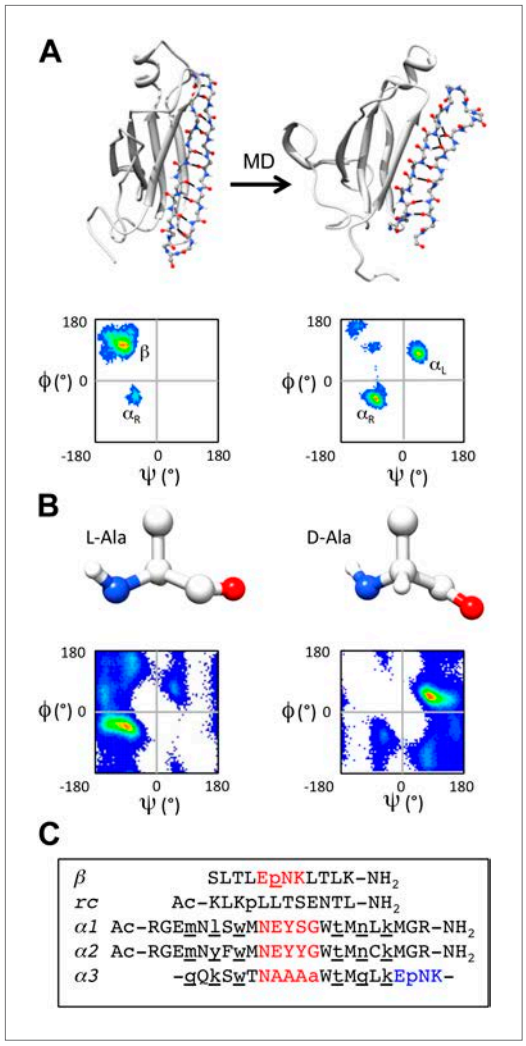

Figure 1. α-sheet conversion, conformational properties and peptide designs. (**A**) β- to α-sheet conversion of transthyretin (as reported by ***Armen et al., 2004a***, ***2004b***). The protein backbone is shown in cartoon representation with the region of interest (residues 105–121) shown as sticks. At 0 ns (top left) the residues of interest form a β-hairpin. The dihedral angles for 1 ns of dynamics of these residues are found mainly in the β-region of the Ramachandran plot (top left quadrant, lower left panel; increasing frequency of occupancy is shown from blue through red) with several turn residues in the α_R conformation (bottom left quadrant). After 30 ns (top right) the β-sheet has converted to an α-sheet. The dihedral angles for 1 ns of dynamics of the same residues reveal that the majority of residues have moved from the β-region to the α_L (top right quadrant) or α_R region of the Ramachandran plot (lower right panel). (**B**) Intrinsic residue propensities for L- and D-alanine were calculated from 100 ns of MD simulations of a GGXGG peptide system (***Beck et al., 2008***) (D-alanine was simulated using the same protocol). The backbone structure (upper panels) as well as the Ramachandran plot of the conformation of the alanine

Figure 1. Continued on next page

Figure 1. Continued

residue during the entire simulation, demonstrate the conformational preference for L-alanine to adopt the α_R conformation and for D-alanine to favor the α_L conformation (lower panels). (**C**) Peptide designs reported in this study. All designs are single turn hairpins, with the exception of *α3*, which contains a cyclic peptide backbone resulting in two turns. Hairpin peptides are N- and C-terminally acetylated and amidated, respectively, except for *β*, which had a free N-terminus. D-amino acids are denoted by lower case and are underlined, and turn residues are colored red in the linear peptides and red and blue in the cyclic design.

DOI: 10.7554/eLife.01681.003

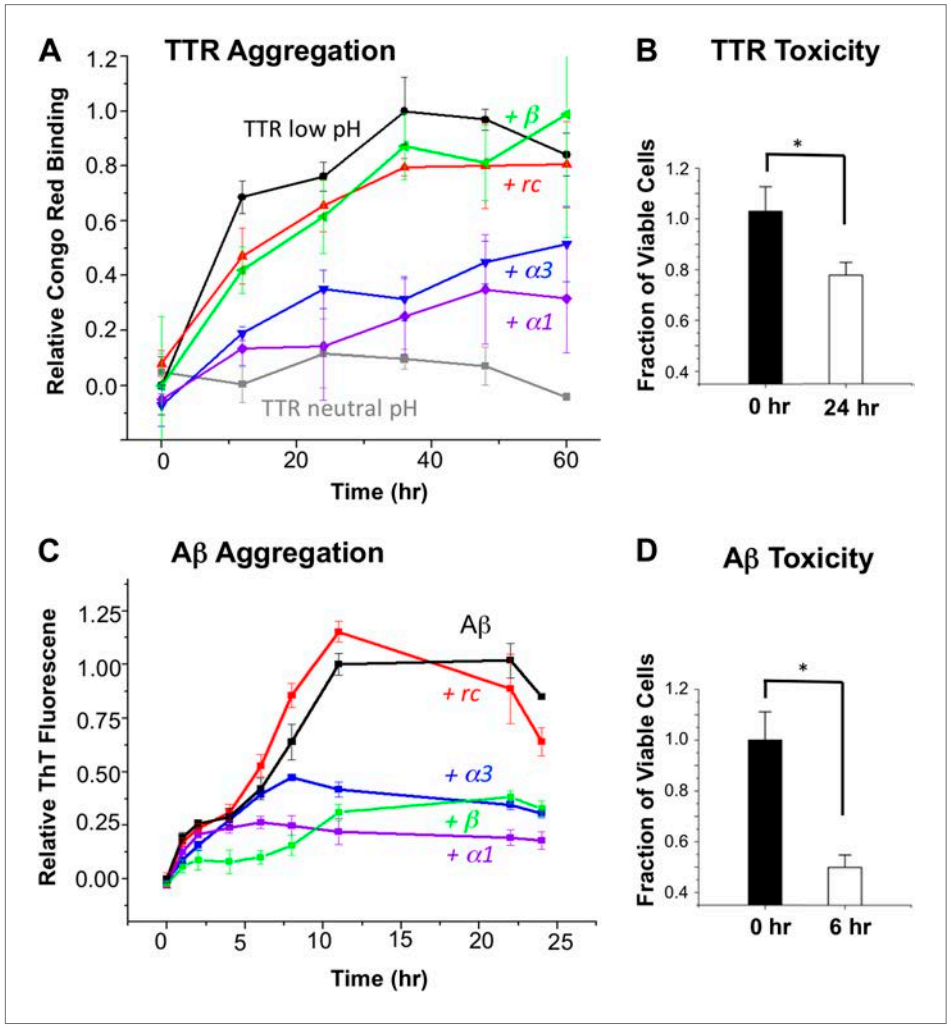

Figure 2. α-Sheet designs inhibit amyloid formation and selectively bind toxic species. (**A**) Peptide designs (800 μM) were co-incubated at pH 4.5 with 40 μM TTR (monomer) at 37°C and aggregation was monitored by Congo red binding. Error bars indicate the standard deviation. (**B**) Toxicity of the TTR solution after 24 hr pre-incubation at pH 4.5 against the human neuroblastoma cell line SH-SY5Y in a MTT metabolic viability assay. (**C**) ThT monitoring of 10 μM Aβ aggregation and inhibitory effects of 100 μM peptides present from the beginning of the aggregation at 37°C. Inhibition values were taken at 12 hr due the decay in ThT fluorescence, particularly for uninhibited samples, which has been described elsewhere (***Yamin et al., 2009***). (**D**) Aβ toxicity after 6 hr of aggregation, as probed using the MTT assay and the SH-SY5Y cell line. All data represent average ± SD (* indicates $p<0.05$, determined using Student's *t* test).

DOI: 10.7554/eLife.01681.004

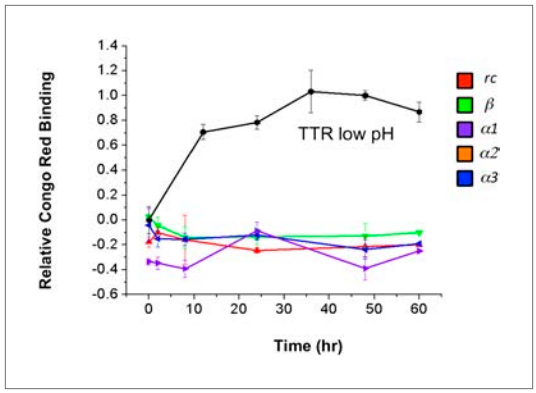

Figure 2—figure supplement 1. Increase in Congo red binding is not due to peptide aggregation.

DOI: 10.7554/eLife.01681.005

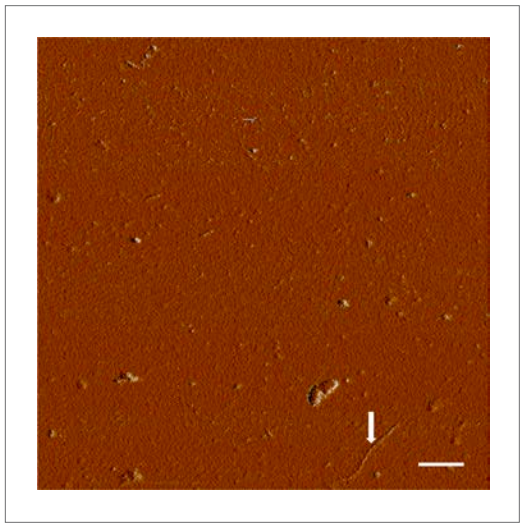

Figure 2—figure supplement 2. AFM spectroscopy reveals aggregation conditions ultimately result in fibrils.

DOI: 10.7554/eLife.01681.006

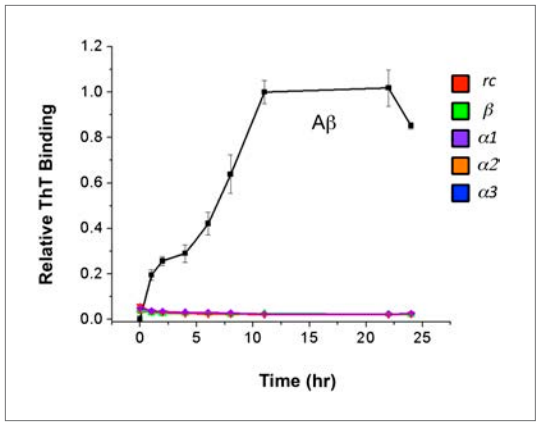

Figure 2—figure supplement 3. Increase in ThT fluorescence is not due to peptide aggregation.
DOI: 10.7554/eLife.01681.007

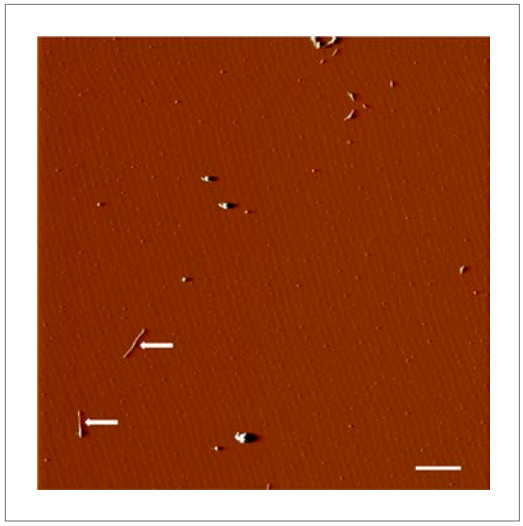

Figure 2—figure supplement 4. AFM spectroscopy confirms an increase in fibrillar products.
DOI: 10.7554/eLife.01681.008

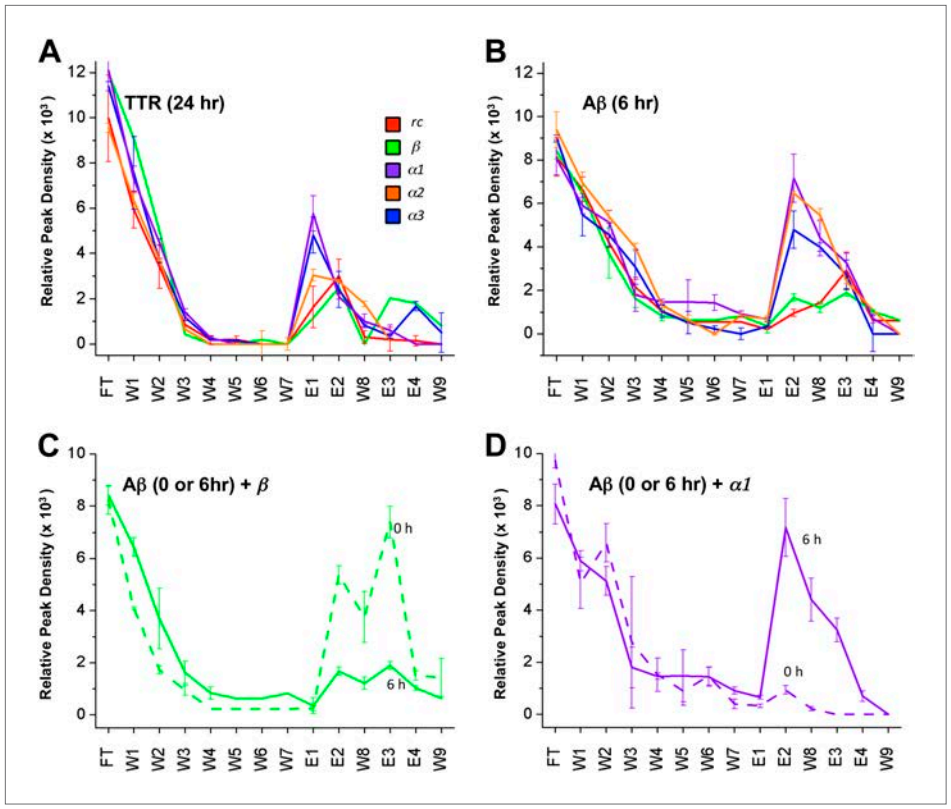

Figure 3. Immobilized designs bind toxic soluble oligomer from solution. Peptide designs were immobilized onto agarose beads and their ability to bind TTR or Aβ from solution at various stages of aggregation was probed using dot blot analysis. The presence of TTR or Aβ in the initial flow through (FT), sequential buffer washes (W), and sequential guanidine hydrochloride elution steps (E1–E2 and E3–E4) (x-axes) was detected by the integrated peak density of the dot blot analysis (y-axes). E1–W9 are within the linear range of the immunochemistry. (**A**) All three α-sheet designs, *α1*, *α2* and *α3* more strongly bound species from the 24 hr pre-aggregated, toxic TTR solutions than did either control. (**B**) Similar results were observed with the α-sheet designs binding to toxic Aβ solutions pre-aggregated for 6 hr. Despite the inhibitory effects seen with the *β* design in the Aβ fibrillization assay, little Aβ from a pre-aggregated solution bound to the immobilized *β* design. (**C**) Comparison of binding from a fresh (0 h), or pre-aggregated (6 hr), toxic Aβ solution. β is the only design that preferentially bound fresh Aβ over the aggregated toxic form, indicating that the inhibition observed was due to interactions with monomeric Aβ. (**D**) In contrast to the β control, α1 preferentially bound the pre-aggregated, toxic form of Aβ compared with fresh monomeric Aβ.
DOI: 10.7554/eLife.01681.009

	TTR (24 hr)				
	rc	*β*	*α1*	*α2*	*α3*
FT	9966 ± 1915	12000 ± 471	12082 ± 888	9555 ± 202	11380 ± 202
W1	5932 ± 812	9087 ± 345	7282 ± 575	6341 ± 309	7554 ± 1614
W2	3420 ± 962	5010 ± 111	4494 ± 139	3714 ± 65	3675 ± 84
W3	855 ± 272	433 ± 144	1403 ± 158	652 ± 72	1197 ± 166
W4	170 ± 188	0	262 ± 61	0	198 ± 32
W5	204 ± 135	0	0	0	142 ± 32
W6	0	195 ± 15	0	0	0
W7	0	0	0	0	0
E1	1630 ± 918	1150 ± 1713	5762 ± 786**	3026 ± 253	4802 ± 793**
E2	2992 ± 747	2500 ± 1429	2088 ± 110	2781 ± 55	2411 ± 796
W8	306 ± 282	0	1014 ± 301**	1774 ± 121**	826 ± 53**
E3	205 ± 532	2032 ± 800	597 ± 241	157 ± 10	355 ± 97
E4	138 ± 229	1800 ± 1320	0	0	1670 ± 202
W9	0	800 ± 40	0	0	506 ± 876
E1+E2+W8	4928 ± 1217	3650 ± 2231	8039 ± 1125**	8864 ± 849**	7581 ± 286**

Figure 3—figure supplement 1. Statistical analysis of data presented in ***Figure 3A***.

DOI: 10.7554/eLife.01681.010

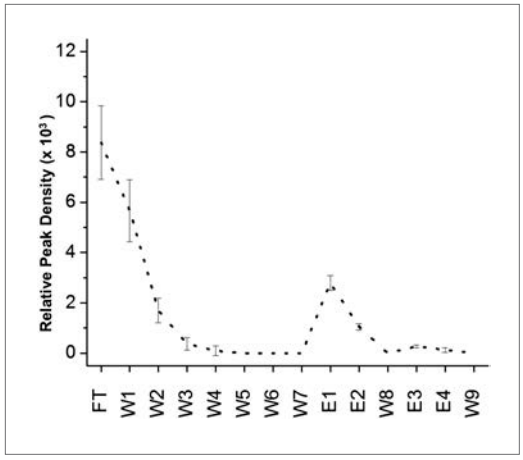

Figure 3—figure supplement 2. Nonspecific binding of nonnative TTR to column matrix.

DOI: 10.7554/eLife.01681.011

	Aβ (6 hr)				
	rc	*β*	*α1*	*α2*	*α3*
FT	8139 ± 881	8410 ± 381	8061 ± 763	9388 ± 823	9026 ± 125
W1	6639 ± 568	6443 ± 350	5891 ± 383	6951 ± 483	5466 ± 976
W2	4179 ± 223	3698 ± 1161	5120 ± 545	5403 ± 267	4545 ± 550
W3	2149 ± 237	1621 ± 428	1798 ± 778	3962 ± 181	3062 ± 793
W4	1045± 20	835 ± 241	1464 ± 116	1340 ± 131	1030 ± 289
W5	551 ± 56	631 ± 43	1472 ± 1000	652 ± 207	507 ± 520
W6	551 ± 23	631 ± 69	1438 ± 364	0	217 ± 144
W7	551 ± 34	822 ± 102	911 ± 130	837 ± 89	100 ± 68
E1	197 ± 162	353 ± 312	657 ± 79	678 ± 141	333 ± 26
E2	959 ± 160*	1666 ± 162*	7160 ± 1110*	6459 ± 89*	4785 ± 859
W8	1438 ± 37	1207 ± 238	4402 ± 825**	5458 ±297**	3970 ± 187**
E3	2914 ± 840	1893 ± 148	3244 ± 454**	2409 ± 102**	2702 ± 678**
E4	604 ± 70	1023 ± 76	700 ± 202	1093 ± 100	0
W9	604 ± 58	631 ± 10	0	0	0
E1+E2+W8	2595 ± 230	3227 ± 424	12219 ± 1385**	12595 ± 341**	9089 ± 879**

Figure 3—figure supplement 3. Statistical analysis of data presented in ***Figure 3B***.
DOI: 10.7554/eLife.01681.012

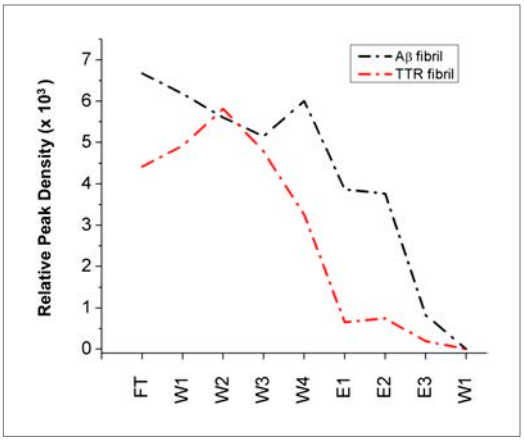

Figure 3—figure supplement 4. Immobilized α-sheet designs do not bind fibrils.
DOI: 10.7554/eLife.01681.013

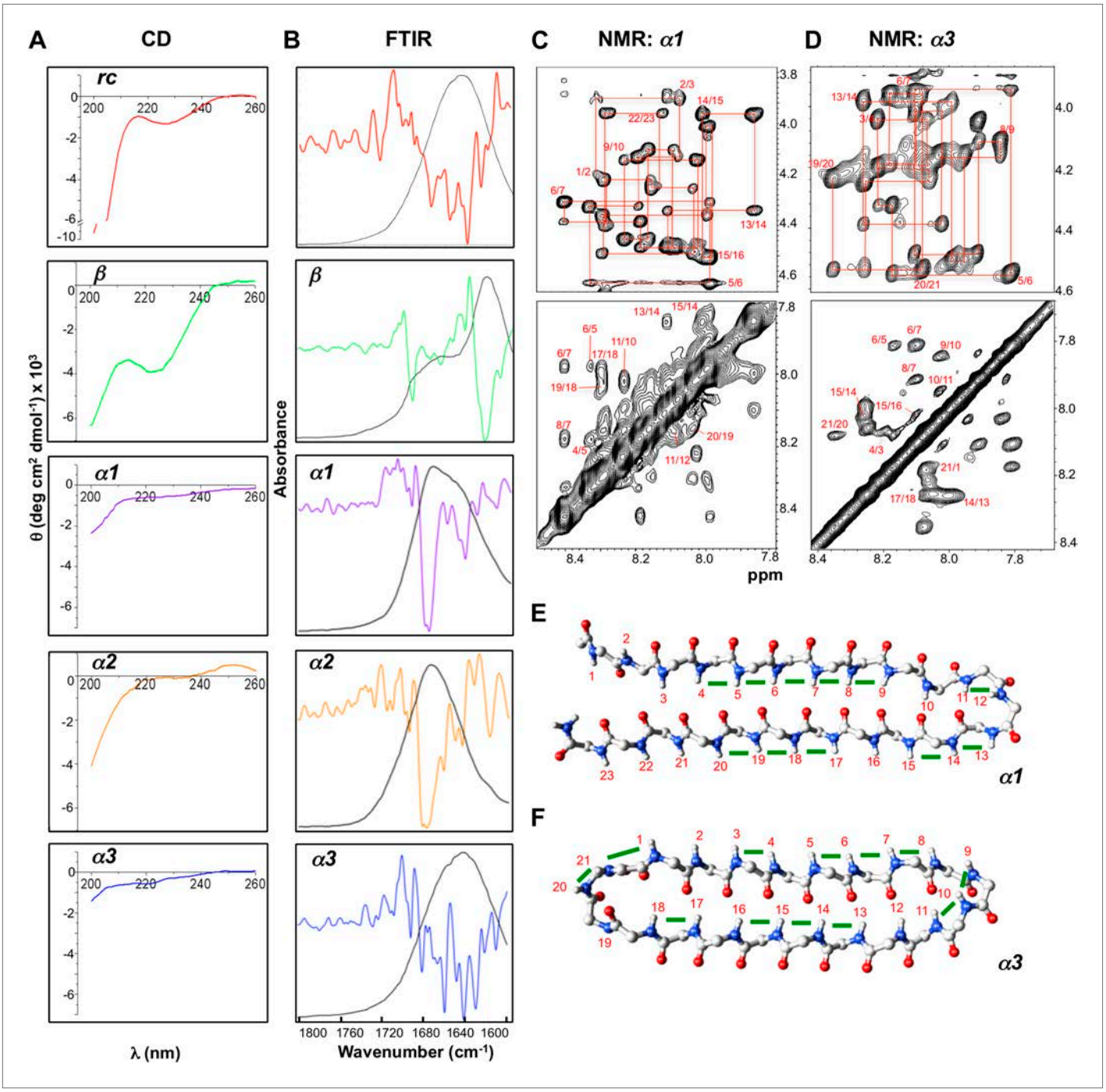

Figure 4. Designed peptides display unique spectroscopic signatures expected for α-sheet. (**A**) CD spectra for peptide designs reveal a random coil structure for *rc* and β-structure spectrum with a bit of random coil for *β*. In contrast, *α1*, *α2* and *α3* have largely featureless CD spectra with some random coil content expected to arise from the turns and tail residues. Note the different scales for the y-axes. All spectra are presented as molar ellipticity, highlighting the difference in intensity of the random coil component for each design compared with the *rc* spectrum. (**B**) FTIR spectra of the peptide designs, displayed as both absorbance (black line) and the second derivative (colored line), correlate well with the CD spectra. The *β* design shows a strong signal at 1632 cm^{-1}, as expected for β-structure. The α-sheet designs have signals near 1640 and 1675–1680 cm^{-1} and the absorption is more intense for *α1 and α2*. (**C**) Fingerprint (top) and NH region (bottom) of the ^{1}H NOESY spectra for *α1*. Sequential assignments are shown in red and multiple sequential NOEs are observed and labeled. (**D**) Fingerprint (top) and NH region (bottom) of the ^{1}H NOESY spectra for *α3*. The NH region reflects the predominance of NH–NH interactions and lack of other main-chain interactions characteristic of the common secondary structures. Mapping backbone NOEs on computational models as green bars (**E**, *α1* and **F**, *α3*) reveal in-plane alignment of the peptide groups along the majority of the

Figure 4. Continued on next page

Figure 4. Continued

sheet. NOEs in the turn regions determined whether the carbonyl or amide hydrogens pointed up in the structures as oriented in the figure (N-terminus top left). Cα, C, N, H and O atoms are shown in gray, gray, blue, white and red, respectively.

DOI: 10.7554/eLife.01681.014

Average H_i-H_{i+1} Distances in α-sheet and β-sheet				
	α1		1QAU	
res #	α-sheet	β-sheet	β-sheet	res #
3	1.88	3.22	4.14	92
4	2.38	2.28	4.64	93
5	2.50	3.22	3.86	94
6	2.77	2.41	4.14	95
7	2.84	4.64	4.14	96
8	2.67	4.64	4.64	97
9	2.51	2.39	4.64	98
10	3.68	3.68	-	99
11	2.41	2.54	-	100
12	2.29	2.00	2.13	101
13	2.16	1.85	2.24	102
14	2.87	4.14	4.64	103
15	2.59	2.43	4.14	104
16	2.62	3.86	4.64	105
17	2.79	4.64	4.14	106
18	2.75	4.14	4.14	107
19	2.79	2.12	4.64	108
20	2.62	2.99	2.26	109
21	2.53	4.14	3.36	110

Figure 4—figure supplement 1. Distances corresponding to d_{NN} NOEs calculated from MD simulations.

DOI: 10.7554/eLife.01681.015

Average Intraresidue $H\alpha_i$-NH_i Distances in α-sheet and β-sheet				
	α1		1QAU	
res #	α-sheet	β-sheet	β-sheet	res #
3	2.98	2.39	2.89	105
4	2.92	2.95	2.99	106
5	2.89	2.28	2.96	107
6	2.85	2.99	2.95	108
7	2.83	2.83	2.88	109
8	2.84	2.82	2.28	110
9	2.91	2.94	2.91	111
10	2.29	2.55	2.89	112
11	2.91	2.96	2.32/2.88	113
12	2.88	2.98	2.81	114
13	2.95	2.99	2.98/2.52	115
14	2.91/2.33	2.74/2.64	2.76	116
15	2.95	2.98	-	117
16	2.93	2.58	2.95	118
17	2.93	2.98	2.27	119
18	2.90	2.88	2.98	120
19	2.91	2.99	2.90	121
20	2.91	2.97	2.99	122
21	2.91	2.28	2.93	123

Figure 4—figure supplement 2. Distances corresponding to intraresidue $d_{\alpha N}$ NOEs calculated from MD simulations.

DOI: 10.7554/eLife.01681.016

Average Sequential $H\alpha_i$-NH_{i+1} Distances in α-sheet and β-sheet

	α1		1QAU	
res #	α-sheet	β-sheet	β-sheet	res #
3	3.52	2.25	2.13	105
4	3.57	3.52	2.18	106
5	3.57	2.18	2.17	107
6	3.57	2.57	2.15	108
7	3.55	2.24	3.55	109
8	3.58	2.15	2.18	110
9	3.49	2.32	2.12	111
10	2.13	2.16	2.63	112
11	3.16	3.52	2.80/3.53	113
12	3.57	3.52	3.55	114
13	3.54	3.12	2.99/3.45	115
14	3.52/2.35	3.18/2.40	-	116
15	3.60	3.17	2.22	117
16	3.61	2.14	3.52	118
17	3.60	2.18	2.12	119
18	3.62	2.17	2.12	120
19	3.61	2.34	2.15	121
20	3.59	3.44	2.16	122
21	3.54	2.18	2.10	123

Figure 4—figure supplement 3. Distances corresponding to sequential $d_{\alpha N\,(i-i+1)}$ NOEs calculated from MD simulations.

DOI: 10.7554/eLife.01681.017